International Journal of Engineering Business Management

OPEN ACCESS
ARTICLE

Application of Bernoulli Process-based Charts to Electronic Assembly

Regular Paper

Darja Noskievičová[1]*, Eva Jarošová[2] and Kateřina Brodecká[3]

1 Department of Quality Management, FMMI, VŠB-TU Ostrava, Ostrava-Poruba, Czech Republic
2 Department of Logistic and Quality Management, Škoda Auto University, Mlada Boleslav, Czech Republic
3 CTS Czech Republic, Ltd. Ostrava, Czech Republic
*Corresponding author(s) E-mail: darja.noskievicova@vsb.cz

Received 21 January 2015; Accepted 05 May 2015

DOI: 10.5772/60758

Abstract

The application of protective gel, which is a subprocess of the electronic assembly of the exhaust gas recirculation sensor, is a highly capable process with the fraction of nonconforming units as low as 200 ppm. Every unit is inspected immediately after gel application. The conventional Shewhart chart is of no use here, and the approach based on the Bernoulli process is therefore considered. The number of conforming items in a row until the occurrence of first or the r-th nonconforming is determined and CCC-r, CCC-r EWMA, and CCC CUSUM charts are applied. The aim of the control is to detect the process deterioration, and so the one-sided charts are used. So that the charts based on the geometric or negative binomial distribution can be compared, their performance is assessed through the average number of inspected units until a signal (ANOS). Our study confirmed that CCC-r EWMA and CCC CUSUM are able to detect the process shift more quickly than the CCC-r chart. Of the two charts, the first is easier to construct.

Keywords CCC-r, CCC-CUSUM, CCC-r EWMA, highly capable process, ANOS

1. Introduction

The statistical process control (SPC) has been widely used in industry, and the control of attribute data represents a considerable part of it. Until recently, the same approach was used to monitor variables or attribute data. In this approach, subgroups of items are taken from a process and sample characteristics are plotted to see whether their variation is only random or whether it is affected by an assignable cause.

When items are classified as conforming or nonconforming, the proportion of nonconforming units in a process (fraction nonconforming) is traditionally monitored by p-chart (or np-chart). Due to new manufacturing technologies and concepts, many processes are of such high quality that the fraction nonconforming or the probability of observing a nonconforming unit is very small. This probability is a parameter of the background binomial distribution, and the size of the subgroups would have to be enormously large to enable the normal approximation, on which the computation of control limits in the conventional control charts is based.

The impossibility of meeting such conditions has the following consequences: real properties of the chart such

as the average run length or the risk of false signal differ from those assuming the normal distribution, and the lower control limit of the p-chart is located at zero and does not enable the recognition of process improvement. Moreover, the appearance of the p-chart containing most zero points is inappropriate. Consequently, the concept based on the sample characteristics is no longer useful for high-quality processes.

Several alternatives based on the Bernoulli process rather than on normal approximation have recently been presented. These methods assume continuous inspection; 100% of these items do not necessarily need to be inspected. For example, Reynolds and Stoumbos in reference [1] admit a situation when 'the production rate is higher than the inspection rate'. In [2] authors also mention an interval sampling, when the items are inspected at scheduled periods. In reference [3] it is emphasized that 'the pattern of the sampling inspection can be quite haphazard without causing any difficulty' for the performance of the control chart studied.

In the Bernoulli process, random variables X_i, $i = 1, 2,...$ express whether an inspected item is conforming or nonconforming. The in-control state of a process is defined by a constant probability p_0 of an occurrence of a nonconforming item. Usually, a sustained shift to the out-of-control state is considered; the process repetitively produces units at level p_0 until it suddenly shifts to an unacceptable level p and remains at this level until a remedial measure is taken.

The situation $p > p_0$ in particular must be detected as soon as possible, and sometimes a minimum value p_1 for p is given. Nevertheless, the inverse inequality $p < p_0$ may also be of interest because it indicates a process improvement.

In [2] the authors consider four groups of methods for monitoring the nonconforming fraction: Shewhart-type charts based on the geometric distribution, Shewhart-type charts based on the negative binomial distribution, CUSUM charts, and EWMA charts also based on the geometric or the negative binomial distribution. The CCC chart representing the first group was designed by Calvin, see [4], and further studied and expanded in [5-7]. The name CCC stands for the cumulative count of conforming units, but more frequently the variable Y that is monitored also includes the immediately following nonconforming unit. Other names such as the conforming run-length CRL in [8] or run-length RL_1 in [6] can be found. We consider the variable Y, and use the inaccurate but more widely known name CCC, in our paper.

To improve sensitivity in detecting small upward shifts in the nonconforming fraction, a chart based on r successive run lengths has been developed. Bourke in [6] first considered RL_2 chart for $r = 2$ with the moving sums $RL_2 = Y_{i-1} + Y_i$ for $i = 2, 3,...$, but later the separated sums $Y_1 + Y_2$, $Y_3 + Y_4$ etc. were used, see e.g., [9].

The more general case $r \geq 2$ is considered in [10-12]. Often r values of 2 or 3 are recommended; see [8] or [13]. In [14] an economic model is constructed to find the best value of r. All of these charts are based on the negative binomial distribution of the monitored variable. A common name for these charts is the CCC-r chart, although other names may appear, e.g., SCRL chart in [8]).

The CCC and CCC-r charts are sometimes called the Shewhart-type charts because of the similar idea of control limit construction, but the geometric or negative binomial distribution is assumed instead of the normal distribution. Besides, their control limits are probability limits, which correspond to the percentiles of an appropriate distribution determined by a chosen risk of a false signal.

Cumulative sum (CUSUM) charts use information from all prior observations, and are considered an efficient alternative to the Shewhart chart when small process shifts are of interest. CUSUM charts can be applied to various distributions, see [15]. As for the Bernoulli process, both the individual observations Xi and the run lengths Yi, defined above can be used. The corresponding CUSUM charts are called the Bernoulli CUSUM or geometric (or CCC) CUSUM, respectively.

Exponentially weighted moving average (EWMA) charts are also based on all prior observations, and have a similar efficiency to the CUSUM charts. The EWMA charts for the Bernoulli and geometric distributions are studied; e.g., in [16], the use of EWMA charts for the negative binomial distribution is suggested [17]. Other references can be found in [2].

Numerous authors have studied the efficiency of these control charts (see further in the paper) but only few case studies have been published; see [18, 19] or [20]. This paper deals with the practical application of various control charts for high yield processes to the highly capable electronic assembling of the exhaust gas recirculation (EGR) valve component. The optimal design and comparative study of statistical properties of CCC-r, CCC CUSUM and CCC EWMA charts with the aim to select the most suitable SPC method for the analysed electronic assembly are the main goals of this study. The paper is organized as follows: at the beginning, all four groups of methods for monitoring the fraction nonconforming based on the Bernoulli process, i.e., Shewhart-type charts based on the geometric distribution, Shewhart-type charts based on the negative binomial distribution, CCC-CUSUM charts and CCC-r EWMA charts, will be described. The ERG sensor and the process of the EGR sensor manufacturing will then be characterized. In the next chapter, optimal parameters of the selected control charts (CCC-r, CCC CUSUM and CCC-r EWMA) will be designed. Then, a comparative study of the selected control charts' efficiency will be performed. Based on this study and application of the chosen control charts, the best alternative will be recommended.

2. SPC Methods for High Yield Processes

As mentioned above, attribute control charts for monitoring and controlling very low fraction nonconforming units based on the Beroulli process can be divided into four groups.

2.1 CCC chart

The variable Y monitored in the CCC chart represents the cumulative count of conforming units to the occurrence of nonconforming unit (often including this immediately following nonconforming units). Determination of the variable Y values monitored in the CCC chart is outlined in Figure 1.

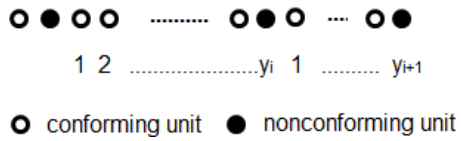

Figure 1. Determination of Y values in CCC chart

Values of runs Y follow the geometric distribution G(p) with the probability function:

$$f(y) = p(1-p)^{y-1}, y = 1, 2, \tag{1}$$

where p is the probability of observing a nonconforming unit in any inspection. The centreline CL in the CCC control chart can be set as the median of the geometric distribution:

$$CL = \frac{\ln\frac{1}{2}}{\ln(1-p)} \tag{2}$$

The two-sided probability control limits (the upper control limit UCL and the lower control limit LCL) are set with the desirable risk of false alarm α, see [21]:

$$UCL = \frac{\ln\frac{\alpha}{2}}{\ln(1-p)}, LCL = \frac{\ln\left(1-\frac{\alpha}{2}\right)}{\ln(1-p)} \tag{3}$$

As these limits are highly asymmetric, the log-scale is sometimes used (for example, see [21]).

As soon as a nonconforming unit is observed the value Yi is plotted in the chart, and counting starts again from zero. The interpretation of such a control chart is quite different from the interpretation of the conventional Shewhart p-chart: the point above UCL means indicates a probable process improvement, and the point below LCL shows probable process deterioration.

When only the upward shift in the process fraction nonconforming is followed, the one-sided lower control limit is given by:

$$LCL = \frac{\ln(1-\alpha)}{\ln(1-p)} \tag{4}$$

2.2 CCC-r chart

Variable Y monitored in the CCC-r chart represents the cumulative count of units until the r-th nonconforming unit is observed – see Figure 2.

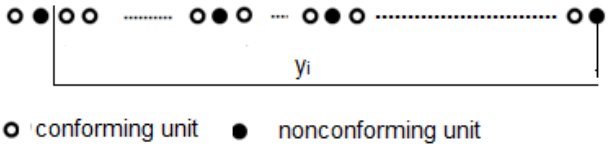

Figure 2. Determination of Y values in CCC-r chart

Y follows the negative binomial distribution with the probability function:

$$f(y) = \binom{y-1}{r-1} p^r (1-p)^{y-r}, y = r, r+1, \tag{5}$$

Assuming that the probability of a nonconforming unit is equal to p, the two-sided control limit and the centreline are determined by solving the following equations; see [22]:

$$F(UCL) = \sum_{y=r}^{UCL} \binom{y-1}{r-1} p^r (1-p)^{y-r} = 1 - \frac{\alpha}{2} \tag{6}$$

$$F(LCL) = \sum_{y=r}^{LCL} \binom{y-1}{r-1} p^r (1-p)^{y-r} = \frac{\alpha}{2} \tag{7}$$

$$F(CL) = \sum_{y=r}^{CL} \binom{y-1}{r-1} p^r (1-p)^{y-r} = \frac{1}{2} \tag{8}$$

When only the upward shift is followed, the one-sided lower control limit must satisfy the equation:

$$F(LCL) = \sum_{y=r}^{LCL} \binom{y-1}{r-1} p^r (1-p)^{y-r} = \alpha \tag{9}$$

for the specified risk of false signal α. The interpretation of the CCC-r chart is similar as in the case of the CCC chart.

When an increase in parameter r, the CCC-r chart is more sensitive to small upward shifts in p. On the other hand, more and more Bernoulli observations are needed to obtain

a point on the chart, and this means that the inspection cost increases (see [14]). For this reason it is necessary to set the optimal parameter r.

2.3 CCC-CUSUM chart

The geometric (or CCC) CUSUM chart (see [6]) is based on the schemes, introduced in [23], expressed by:

$$\begin{aligned} S_i^+ &= \max\left(0, S_{i-1}^+ + y_i - K^+\right) \\ S_i^- &= \min\left(0, S_{i-1}^- + y_i - K^-\right) \; i = 1, 2, \end{aligned} \tag{10}$$

where y_i is a value of Y that follows the geometric distribution G(p) and K^+ (K^-) is a constant. Often $S_0 = 0$ is used, but a head start can be chosen to quickly detect an initial out-of-control state; see [6].

Only the lower scheme used to detect an upward process shift is considered here. If the process deteriorates, i.e., when the fraction nonconforming p increases, values y_i less than K^- predominate and S_i^- becomes more and more negative. As soon as S_i^- drops under a specified limit H^- for some i, an out-of-control signal is given. The value of H^- determines the chart performance: the more negative it is, the longer the time to the signal.

When a shift from the in-control p_0 to a higher value p is to be detected, the minimum value p_1 that is considered inappropriate must be chosen. If $p \le p_0$, the level of the fraction nonconforming is acceptable; if $p \ge p_1$, the level is unacceptable. As a matter of the fact, hypotheses H_0: $p = p_0$ versus H_1: $p = p_1$ are tested. H_0 is rejected when S_i^- is less than H^-.

2.4 CCC-r EWMA chart

The exponentially weighted moving average (EWMA) is defined as:

$$z_t = \lambda y_t + (1-\lambda) z_{t-1} \tag{11}$$

where $0 < \lambda \le 1$ is a smoothing constant and the starting value $z_0 = y_0$ is usually the process target. The construction of EWMA control limits is based on normal distribution, but it is known that the EWMA chart is quite robust to non-normality [24]. The control limits of the EWMA chart are:

$$UCL_i = y_0 + L\sigma_Y \sqrt{\frac{\lambda}{2-\lambda}\left[1-(1-\lambda)^{2i}\right]} \tag{12}$$

$$LCL_i = y_0 - L\sigma_Y \sqrt{\frac{\lambda}{2-\lambda}\left[1-(1-\lambda)^{2i}\right]} \tag{13}$$

where L denotes a constant determining the distance between the limits, and consequently the chart performance. Due to the fact that the term $[1-(1-\lambda)^{2i}]$ approaches unity as i gets larger, sometimes the steady-state limits are given as follows:

$$UCL^* = y_0 + L\sigma_Y \sqrt{\frac{\lambda}{2-\lambda}} \tag{14}$$

$$LCL^* = y_0 - L\sigma_Y \sqrt{\frac{\lambda}{2-\lambda}} \tag{15}$$

For $Y \sim$ NB(p, r) the target value is:

$$y_0 = E(Y) = \frac{r}{p_0} \tag{16}$$

and the standard deviation of the in-control process is:

$$\sigma_Y = \frac{\sqrt{r(1-p_0)}}{p_0} \tag{17}$$

3. Electronic Assembly Description

The methods described in the previous chapter were applied to the highly capable process of EGR sensor manufacturing. The current cars contain numerous electronic parts with various functions. The EGR valve is a part of the combustion motor which greatly reduces nitrogen oxide (NOx) emissions and therefore helps to protect the environment. One of the components enabling control of the EGR valve is the EGR pressure sensor, which detects the exhaust gas flow. The electronic assembly of the EGR sensor consists of several subprocesses - see Figure 3.

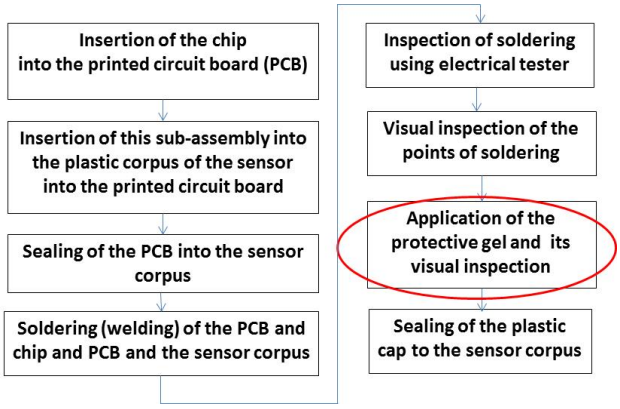

Figure 3. Structure of the electronic assembly of the EGR sensor

The last but one subprocess is the manual application of the protective gel. The amount of gel is given by the dosing device. The operator presses the pedal and so applies the predetermined amount of the gel. Every sensor is visually inspected – this means that the continuous 100% inspection is carried on. The difference between a conforming and nonconforming unit can be seen in Figure 4 and 5. The gel

must not get to the groove for the following ultrasonic sealing of the plastic sensor cap. Each sensor with the gel in this groove is considered to be the nonconforming unit that must be separated. This subprocess works with in-control fraction nonconforming $p_0 = 0.0002$ (200 ppm) [25].

Figure 4. Conforming unit [25]

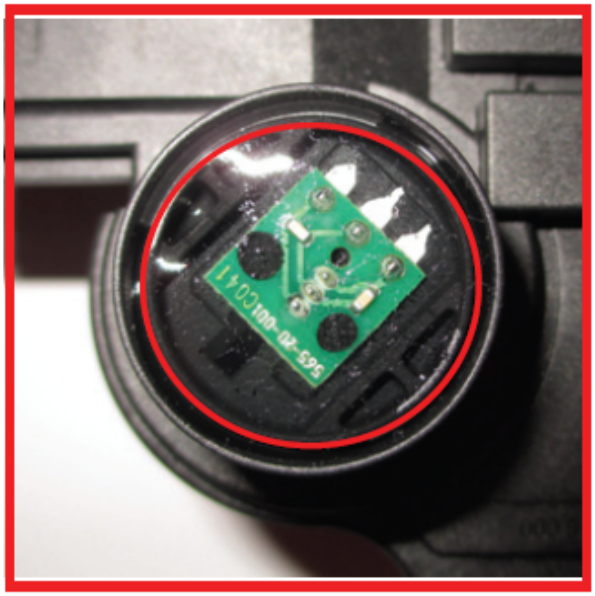

Figure 5. Nonconforming unit [25]

To keep the fraction nonconforming at such a low level, or to lower the process, it has to be controlled; therefore, a suitable control chart for this capable process should be chosen.

4. Design of Parameters for Selected Control Charts

Based on the analysis of the EGR sensor electronic assembly it the application of CCC-r charts, CCC CUSUM and CCC-r EWMA charts was decided. For each type of control chart, parameters corresponding to the process in-control $p_0 = 0.0002$, out-of-control fraction of nonconforming $p_1 = 0.001$ and various risks of false signal ($\alpha = 0.01$, 0.005 and 0.002) were set.

4.1 Design of CCC-r charts

Optimal values of parameter r for the conditions of the analysed electronic assembling were set using the new semi-economic model designed in [25]. This semi-economic model is based on the economic design of the CCC-r chart described in [14] but is easier to apply in practice. The model is based on the idea that by increasing parameter r the CCC-r chart becomes more sensitive to small changes in the proportion of nonconforming units p, but on the other hand a greater r increases the costs of testing and inspection. The algorithm of the new semi-economic model is based on the minimization of the overall expected costs $E(C)$ consisting of the expected costs induced by the production of nonconforming units $E(NJ)$ and the expected costs of inspection and testing $E(KT)$. Only the parameter r is optimized. Costs $E(NJ)$ and $E(KT)$ can be computed using the following formulae:

$$E(NJ) = g_1 E(A_1) hv \tag{18}$$

$$E(KT) = aE(Y) \tag{19}$$

where

g_1.....is the unit production cost when the process is not statistically stable;

$E(A_1)$.... is the expected number of units produced when the process is not statistically stable;

h.....is the control interval length;

v.....is the number of produced units per operation time unit;

a.....is the unit testing cost;

$E(Y)$.....is the expected number of units inspected until the occurrence of the r-th nonconforming unit.

The input parameters for the semi-economic model were derived or computed from the production records: the proportion of nonconforming units when the process is statistically stable was set as $p_0 = 0.0002$, the unacceptable proportion of nonconforming units was $p_1 = 0.0010$, the unit production cost at p_1 was $g_1 = 95$ CZK, the unit testing and inspection cost $a = 0.3397$ CZK, the control interval length $h = 0.003$ h, the number of units produced per operation time unit $v = 315$ units [25]. Considering three values of the risk of false signal α led to two values of the parameter r and three different values of the lower control limit LCL (see Table 2 in paragraph 4.4).

4.2 Design of CCC CUSUM

The parameters K^- and H^- can be derived from the Wald sequential probability test [26] when the geometric distribution (1) is considered. The reference value K^- depends on the target value p_0 and the unacceptable value p_1 of the fraction nonconforming:

$$K^- = \frac{\ln \dfrac{p_1(1-p_0)}{p_0(1-p_1)}}{\ln \dfrac{1-p_0}{1-p_1}} \tag{20}$$

The lower control limit H^- is approximately:

$$H^- = \frac{-\ln \alpha}{\ln \dfrac{1-p_0}{1-p_1}} \tag{21}$$

In fact, the use of this value does not imply ANOS(p_0) equal to $1/\alpha$. To reach a value that is nearer to a specific ANOS(p_0), the approximate method by Reynolds and Stoumbos [1] for the Bernoulli CUSUM chart can be used. Based on the relationship between the Bernoulli and geometric distribution, the lower limit for the CCC CUSUM chart can be derived.

The approximate in-control average number of observations for the one-sided Bernoulli CUSUM chart ($p_1 > p_0$ is assumed) is given by:

$$ANOS(p_0) \approx \frac{\exp(H_B^* r_2) - H_B^* r_2 - 1}{\left| r_2 p_0 - r_1 \right|} \tag{22}$$

where

$$r_1 = -\ln\left(\frac{1-p_1}{1-p_0}\right)$$

$$r_2 = \ln\left(\frac{p_1(1-p_0)}{p_0(1-p_1)}\right)$$

$$H_B^* = H_B^- + \varepsilon(p_0)\sqrt{p_0(1-p_0)}$$

$$\varepsilon(p_0) \approx \begin{cases} 0.410 - 0.0842\ln p_0 - 0.0391(\ln p_0)^3 - \\ -0.00376(\ln p_0)^4 - 0.000008(\ln p_0)^7 \\ \qquad\qquad \text{if } 0.01 \le p_0 \le 0.5 \\ \left(\sqrt{(1-p_0)/p_0} - \sqrt{p_0/(1-p_0)}\right)/3 \\ \qquad\qquad \text{if } 0 < p_0 < 0.01 \end{cases}$$

First, H_B^* is obtained from (20), e.g., by means of the Excel function *Goal Seek*. Once the parameter H_B^- of the Bernoulli CUSUM chart has been found, the lower limit H_G^- of the geometric CUSUM chart can be expressed as:

$$H_G^- = -m(H_B^- - 1) \tag{23}$$

where $m = \lfloor K^- \rfloor$, i.e., K^- rounded down, see [27]).

4.3 Design of CCC-r EWMA

The parameters λ and L are chosen in the same way as in the case of a normal distribution. Based on the assumption of normality, Crowder in [28] constructed nomograms that can be used for the choice of λ and L to obtain the optimal combination, in the sense that for a fixed risk of false signal α and for a specified shift δ the ARL is the smallest possible. With reference to the robustness of the EWMA chart, these curves have been used for the design of the CCC-r EWMA chart.

To make use of the nomograms by Crowder in the case of the distribution NB(p,r), the shift in the mean in multiples of the standard deviation is expressed by:

$$\delta = \frac{\dfrac{r}{p_0} - \dfrac{r}{p_1}}{\sqrt{r\dfrac{1-p_0}{p_0^2}}} = \sqrt{\frac{r}{1-p_0}}\left(1 - \frac{p_0}{p_1}\right) \tag{24}$$

For a given δ and some chosen ARL(0), which is related to ANOS(p_0) according to:

$$ARL(0) = ANOS(p_0)\frac{p_0}{r} \tag{25}$$

values of λ and L can be successively read in the nomograms. As the use of nomograms gives only approximate values, the nomograms can only be used to find λ and L; the values of ARL for some non-zero δ can also be determined. In this paper the nomograms were used only for λ determination and the value of L; the corresponding ARL was obtained through the procedure for EWMA charts using Statgraphics Centurion computer software.

Consistently with the previous control charts, only the one-sided lower limit of the CCC-r EWMA chart was considered (see Table 1, paragraph 4.4). The same values of r as in the CCC-r charts were used.

4.4 Results

Based on different values of the input parameters α, p_0, p_1 and the corresponding chart parameters r, K,λ and L (see Table 1) three control charts of each type were obtained.

α	r	CCC-r	CCC-r EWMA			CCC-CUSUM	
		LCL	λ	L	LCL^*	K^-	H_G^-
0.01	2	744	0.23	2.10	4648	2011	–5044
0.005	2	518	0.20	2.35	4462	2011	–5901
0.002	3	1217	0.25	2.75	5999	2011	–7545

Table 1. Designed optimal parameters of the control charts

All nine variants of the control charts were constructed and applied to the data from the analysed electronic assembly, see Figure 6 – 11.

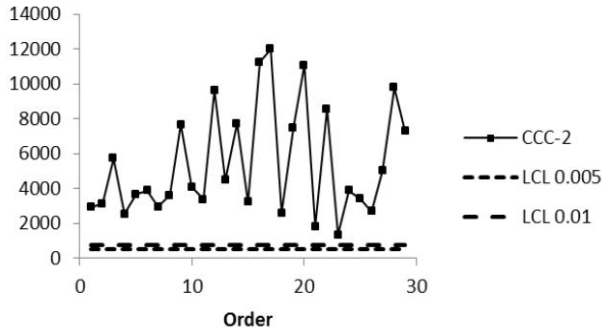

Figure 6. CCC-2 chart (α = 0.005 and 0.01)

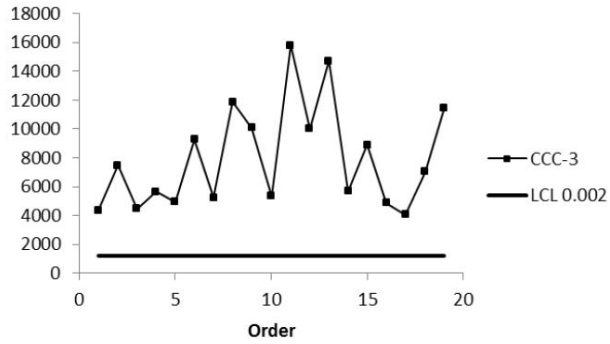

Figure 7. CCC-3 chart (α = 0.002)

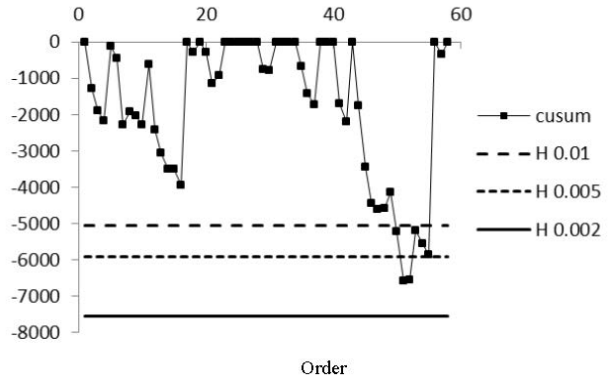

Figure 8. CCC-CUSUM chart (α = 0.002; 0.005; 0.01)

It can be seen that only CCC-CUSUM for α = 0.01 or α = 0.005 and CCC-2 EWMA for α = 0.01 indicate the process

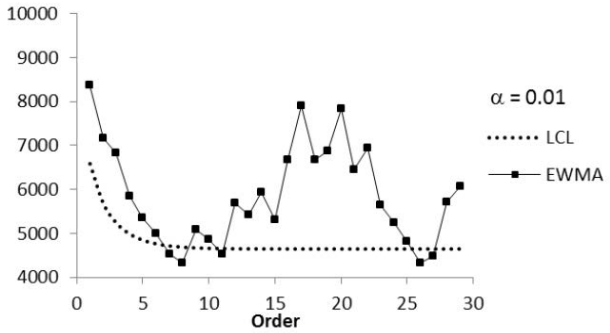

Figure 9. CCC-2 EWMA chart (α = 0.01)

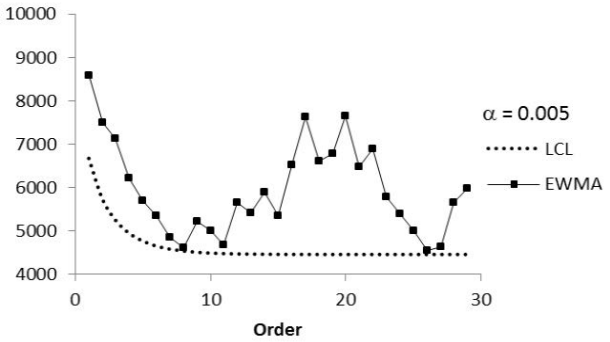

Figure 10. CCC-2 EWMA chart (α = 0.005)

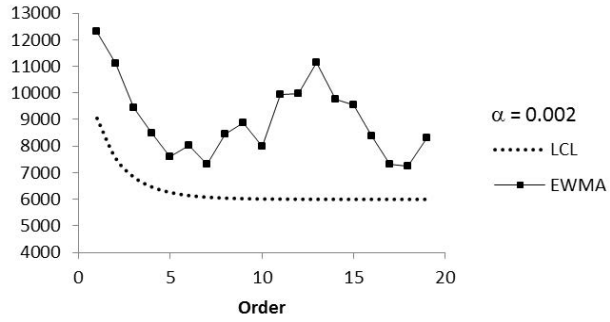

Figure 11. CCC-3 EWMA chart (α = 0.002)

instability after the 50th, 51st, and 52nd nonconforming item, respectively. In addition, CCC-2 EWMA gives an earlier signal after the 14th nonconforming item. A closer comparison of these control charts efficiency will be made in the next chapter.

5. Comparison of the Designed Charts Performance

When the performance of different types of control charts is to be compared, a suitable criterion must be chosen. For the classical Shewhart, CUSUM or EWMA charts, when both the sample sizes and the sampling intervals are equal, the average run length ARL can be used. This represents the expected number of samples before the first signal occurs. This measure is inappropriate when different types

of charts, based on the Bernoulli process, are compared. The observations y_i correspond to different numbers of inspected units, and this fact must be taken into consideration; this is why another measure has been introduced. In [1] the average number of observations to signal ANOS that represents the expected number of inspected items to the signal is used. The average time to signal ATS, the average number inspected ANI, and the average number of items sampled ANIS, are different names for the same measure used; see [6, 8, 19]. It is common to compare the efficiency of charts that have roughly equal ANOS(p_0) (i.e., ANOS when the process is statistically stable); see e.g., [1] or [8]. The efficiency is evaluated by means of $ANOS(p_1)$ (i.e., ANOS when the proportion of nonconforming is p_1), which should be as small as possible.

The values of ANOS for CCC-r charts were determined according to:

$$ANOS(p) = \frac{r}{p \cdot F(LCL)} \tag{26}$$

To evaluate the ANOS for CCC-CUSUM chart, either an approach based on a Markov chain or the approximate method published in [1] and mentioned already in 4.2 can be used. In addition to ANOS(p_0) given by (22), formulae for ANOS(p_1) and ANOS(p^*), where $p^* = r_1/r_2$ are used in this study:

$$ANOS(p_1) \approx \frac{\exp(-H_B^* r_2) + H_B^* r_2 - 1}{|r_2 p_1 - r_1|} \tag{27}$$

$$ANOS(p^*) \approx \frac{H_B^* (H_B^* + p^*) r_2^2}{r_1 (r_2 - r_1)} \tag{28}$$

The ANOS for CCC-r EWMA is obtained by:

$$ANOS(p) = ARL(p)\frac{r}{p} \tag{29}$$

Values of ARL(δ) for the common EWMA chart are obtained by solving integral equations, see [29], and Statgraphics Centurion can be used to find them. ARL(p_1) and ARL(p^*) for the CCC-r EWMA were determined identically. In the case of ARL(p_1) δ was given by (24); for determining ARL(p^*) the proportion p_1 in (24) was replaced by p^*. The values of ARL(p) are only approximate. Apart from the non-normal distribution another issue had to be taken into account; ARLs obtained by means of either the nomograms or Statgraphics Centurion are two-sided. It is expected that the one-sided and two-sided ARLs will be approximately the same for larger δ, say about 1 and greater. In this sense the values of ANOS (p^*) for α = 0.01 and 0.005 in Table 2 (denoted by *) are slightly underestimated due to the fact that δ was equal to 0.845 in these cases. As for ARL(0), half of the value implied from (25) was considered for a given ANOS(p_0).

Values of $ANOS(p_0)$, $ANOS(p_*)$ and $ANOS(p_1)$ for all nine designed control charts are summarized in Table 2.

α	Control chart	ANOS(p_0) p_0 =0 .0002	ANOS(p_*) p^* =0.0005	ANOS(p_1) p_1 =0.001
0.01	CCC-2	1 000 511	74 023	11 707
	CCC-2 EWMA	1 000 000	28 400*	9 800
	CCC-CUSUM	1 000 000	29 701	6 406
0.005	CCC-2	2 006 896	142 157	20 980
	CCC-2 EWMA	2 000 000	35 200*	11 600
	CCC-CUSUM	2 000 000	36 658	7 253
0.002	CCC-3	7 515 595	251 278	24 210
	CCC-3 EWMA	7 500 000	51 600	15 900
	CCC-CUSUM	7 500 000	52 044	8 877

Table 2. ANOS values

The $ANOS(p_1)$ of the CCC-CUSUM is the best, regardless of the value of the risk α. The $ANOS(p_1)$ of the CCC-r chart is much larger and the worst. Although the CCC-r EWMA chart detects shifts to the chosen p_1 more slowly than the CCC-CUSUM, smaller shifts may be detected rather more quickly; see the column for p^*. The pattern in Figure 5 corresponds to this feature.

6. Conclusions

Design of the optimal parameters of control charts suitable for controlling the highly capable subprocess of ERG sensor electronic assembly and the comparative analysis of the designed control chart efficiency (i.e., CCC-r, CCC-r EWMA and CCC-CUSUM charts), with the aim of recommending the best control charting method, were the main goals of this paper.

Our study confirmed that the CCC-r EWMA and CCC CUSUM charts are able to detect a process shift much more quickly than the Shewhart type CCC-r chart. The only advantage of the last type is its more simple construction. Under the assumption that both former charts are designed with regard to the smallest unacceptable proportion of nonconforming units p_1 = 0.001, the CUSUM chart gives an earlier signal when a process shift corresponds to this level. When a smaller shift occurs, the CCC-r EWMA chart may react faster, as is indicated by ANOS for p = 0.0005. As a

matter of fact, this feature of the CCC-r EWMA chart could be rather redundant in operations where the proportion p is acceptable unless the value p_1 is crossed, as in this case the signal might be considered a false alarm.

Based on the ANOS measure, it can be concluded that the CCC-CUSUM chart is the best choice for this electronic assembling process. Consider charts with ANOS(p_0) = 1,000,000 and the shift from p_0 = 0.0002 to p_1=0.001: with the CCC-2 chart 11 707 0.001 = 11.7 nonconforming units can be expected, compared to 11 707 0.0002 = 2.3 units in the process without the shift. The expected number of nonconforming units until the signal is higher by 9.4. Using the CCC-2 EWMA chart and the CCC CUSUM chart we get 7.8 and 5.1, respectively. It follows that with the CCC CUSUM, the cost incurred by producing a larger number of nonconforming units after the shift is slashed by 45% compared with the CCC-2 chart. Considering the two larger ANOS(p_0), the cost is reduced even by 65% (63%).

7. Acknowledgements

This paper was elaborated in the frame of the specific research project SP2015/112 which has been solved at the Faculty of Metallurgy and Materials Engineering, VŠB-TU Ostrava with the support of the Ministry of Education, Youth and Sports, Czech Republic, and by the project ŠKODA AUTO a.s., IGA/2012/9.

8. References

[1] Reynolds M.R, Stoumbos Z.G (1999) A CUSUM Chart for Monitoring a Proportion When Inspecting Continuously. J. qual. technol. 31: 87–108.

[2] Szarka J.L.III, Woodall W.H (2011) A Review and Perspective on Surveillance of Bernoulli Processes. Qual. reliab. eng. int. 27: 735-752.

[3] Bourke P.D (2001) The Geometric CUSUM chart with Sampling Inspection for Monitoring Fraction Defective. J. appl. stat. 28: 951–972.

[4] Calvin T (1983) Quality Control Techniques for Zero Defects. IEEE Transactions on components hybrids and manufacturing technology 6: 323-328.

[5] Goh T.N (1987) A Control Chart for Very High Yield Processes. Qual. assur j. 13: 18-22.

[6] Bourke P.D (1991) Detecting a Shift in Fraction Nonconforming using Run-Length Control Charts with 100% Inspection. J. qual. technol. 23: 225-238.

[7] Xie W, Xie, M, Goh T.N (1995) A Shewhart-like Charting Technique for High Yield Processes. Qual. reliab. eng. int. 11: 189-196.

[8] Wu Z, Yeo S.H, Fan H (2000) A Comparative Study of the CRL–Type Control Charts', Qual. reliab. eng. int. 16: 269–279.

[9] Wu Z, Zhan X, Yeo S.H (2001 Design of the Sum–of–Conforming–Run–Length Control Charts. Eur. j. oper. res. 132: 187–196.

[10] Xie M, Lu, X.S, Goh T.N, Chan, L.Y (1999) A Quality Monitoring and Decision-making Scheme for Automated Production Processes. Int. j. qual. reliab. manag. 16: 148-157.

[11] Kaminsky F.C, Benneyan J.C, Davis R.D, Burke R.J (1992) Statistical Control Charts Based on a Geometric Distribution. J. qual. technol. 24: 63–69.

[12] Xie M, Goh, T.N (1997) The Use of Probability Limits for Process Control Based on Geometric Distribution. Qual. reliab. eng. int. 14: 64-73.

[13] Schwertman N.C (2005) Designing Accurate Control Charts Based on the Geometric and Negative Binomial Distribution. Qual. reliab. eng. int. 21: 743-756.

[14] Ohta H, Kusukawa E, Rahim A (2001) A CCC-r Chart for High-Yield Processes. Qual. reliab. eng. int. 17: 439-446.

[15] Hawkins D.M, Olwell D.H (1998) Cumulative Sum Charts and Charting for Quality Improvement. New York: Springer. 247p.

[16] Yeh A.B, McGrath R.N, Sembower M.A, Shen Q (2008). EWMA Control Charts for Monitoring High-yield Processes Based on Non-transformed Observations. Internat. j. prod. res. 46: 5679-5699.

[17] Kotani T, Kusukawa E, Ohta, H (2005) Exponentially Weighted Moving Average Chart for High-Yield Processes. An international journal of industrial engineering and management systems 4, 1: 75-81.

[18] Di Bucchianico A, Mooiweer G.D, Moonen E.J.G (2005) Monitoring Infrequent Failures of High-volume Production Processes. Qual. reliab. eng. int. 21: 521-528.

[19] Chang T.C, Gan F.F (2001) Cumulative Sum Charts for High Yield Processes. Stat. sinica 11: 791–805.

[20] Rashid K.M.J, Rahi A.R. (2012) Using Cumulative Count of Conforming CCC-Chart to Study the Expansion of the Cement. IOSR J 2: 51-60.

[21] Xie M, Goh T.N, Kuralmani C (2002) Statistical Models and Control Charts for High Quality Processes. Norwel, Massachusetts: Kluwer Academic Publishers. 273p.

[22] Chen P.W, Cheng Ch.S (2010) An ARL-Unbiased Approach to Setting Control Limits of CCC-r Chart for High Yield Processes. Journal of quality 17: 435-451.

[23] Page, E.S (1961) Cumulative Sum Charts. Technometrics 3: 1–9.

[24] Montgomery D.C (2009). Statistical Quality Control: A Modern Introduction. Hoboken: J. Wiley & Sons. 734p.

[25] Brodecká K (2013) Application of Selected Statistical Methods at Conditions of High Yield Processes (in Czech). Doctoral Thesis. Ostrava: VŠB-TU Ostrava.

[26] Wald A (1945) Sequential Tests of Statistical Hypotheses The annals of mathematical statistics 16: 117–186.

[27] Szarka J.L.III, Woodal W.H (2012) On the Equivalence of the Bernoulli and Geometric CUSUM Charts. J. qual. technol. 44: 54–62.

[28] Crowder S.V (1989) Design of Exponentially Weighted Moving Average Schemes. J. qual. technol: 155–162.

[29] Crowder S.V (1987) A Simple Method for Studying Run-Length Distribution of Exponentially Weighted Moving Average Control Charts. Technometrics 29: 401–407.